The EMBO Journal vol.4 no.9 pp.2389-2395, 1985

Characteristic views of *E. coli* and *B. stearothermophilus* 30S ribosomal subunits in the electron microscope

Marin van Heel and Marina Stöffler-Meilicke[1]

Fritz-Haber-Institut der Max-Planck Gesellschaft, Faradayweg 4-6, and [1]Max-Planck-Institut für Molekulare Genetik, Abt. Wittmann, Ihnestrasse 63-73, D-1000 Berlin-Dahlem, FRG

Communicated by R.Henderson

Large sets of electron microscopic images of the 30S ribosomal subunits of *Bacillus stearothermophilus* (914 molecules) and *Escherichia coli* (422 molecules) were analysed with image processing techniques. Using computer alignment and a new multivariate statistical classification scheme, three predominant views of the subunit were found for both species. These views, which together account for ~90% of the population of images, were determined to a reproducible resolution of up to 1.7 nm, thus elucidating many new structural details. The angular spread of the molecular orientations around the three main stable positions is remarkably small (<8°). Some of the current models for the small ribosomal subunit are incompatible with our new results.

Key words: automatic classification/electron microscopy/image analysis/multivariate statistical analysis/ribosome structure

Introduction

Electron micrographs of biological macromolecules are usually very noisy and are hence difficult to interpret visually. Random variation in the stain distribution around the molecules is one of the major sources of noise. Averaging of images of different molecules is a technique that can be used to suppress the contribution of the (random) noise relative to that of the (common) signal and thereby enhance the statistical significance (signal-to-noise ratio: SNR) of the results. Image averaging techniques for macromolecules arranged in regular arrays (two-dimensional crystals or helices) were developed by Klug and co-workers (DeRosier and Klug, 1968). Reproducible resolutions down to ~0.7 nm have been reached (Unwin and Henderson, 1975). Techniques to align and average images of individual molecules were developed later (cf. Frank *et al.*, 1981). A fundamental problem with this approach is, however, that single molecules can lie in different orientations on the support film and this has to be taken into account prior to averaging. A significant step towards the solution of this problem was the introduction of multivariate statistical analysis (MSA) methods, namely correspondence analysis (Van Heel and Frank, 1981), which leads to a large reduction of the total data volume and thus facilitates the understanding of the data set.

Nonetheless, it is the next phase, the decision-making or classification phase, which embodies the artificial intelligence of the procedure. We have to group images in a logical way so as to elucidate the properties of the population of images. An automatic classification scheme based on sound criteria is indispensable to obtain an objective partitioning (Van Heel, 1984a). The noise-free class averages thus obtained reflect the molecule in its various stable positions so that it becomes possible to analyse mixed populations of images like the 'randomly oriented' 30S ribosomal subunits.

Most published models of the 30S ribosomal subunit of *Escherichia coli* are based on subjective interpretation of electron microscopical images (Tischendorf *et al.*, 1974,1975; Lake, 1976; Shatsky *et al.*, 1979; Boublik *et al.*, 1977; Stöffler and Stöffler-Melicke, 1983). The noisy images were classified and interpreted by eye; hence it is not surprising that the various models for the subunit differ considerably. In the current paper we use our multivariate statistical classification techniques to find the characteristic views of the 30S subunit from *E. coli* and *Bacillus stearothermophilus*, which can provide a more objective data base for the construction of three-dimensional models.

Results

Bacillus stearothermophilus

The 914 aligned images of *B. stearothermophilus* were partitioned into 30 different classes (Figure 2) by the classification algorithm. To illustrate the sorting power of the technique, a number of class-averages are shown in Figure 3 together with some of the (aligned) original images of which they consist. A number of the classes in Figure 2 were considered to be insignificant (Figure 2F) on the basis of their high internal variance; they contain misaligned or uncharacteristic images. The good classes (Figure 2A – E) are shown sorted by characteristic view; these classes represent >90% of the total population (5% were rejected during the hierarchical ascendent classification (HAC) procedure, an additional 5% fell into the insignificant classes, not including the misaligned ones). The classes comprising a characteristic view are sorted mainly by the number of member images. Most images fall into two predominant views, the 'asymmetric' or 'lateral' view (32%, Figure 2A) and the 'intermediate' view (39%, Figure 2B). The three other less-frequent views are the well-known 'quasi-symmetric' view (10.4%, Figure 2C) and two variants of the latter, a compact view (2.8%, Figure 2D) and a curved view (3.3%, Figure 2E). The compact variant is considerably shorter than the other views and is likely to be a position in which the long axis of the particle is not parallel to the support film; it tends to be surrounded by a stain layer thicker than in the other views.

It is remarkable that the lateral view is seldom observed in the left-handed position (2.6% of total population). Furthermore, of the 21 left-handed lateral view images present in the series, 17 are found in just two micrographs (which also contain 36 right-handed ones), indicating local differences in preparation conditions. The other views are exclusively present in one version, with the mirror views missing completely.

The lateral view of *B. stearothermophilus* shows a beak-like structure at the head of the particle (Figure 2A), and in both the lateral and the intermediate view, the base of the 30S subunit is squarish rather than round (Figure 2A, B). All classes within one view show largely the same details. For example, all lateral views show a characteristic pattern of three small protrusions at the side of the large lobe (Figure 2A). In the intermediate view,

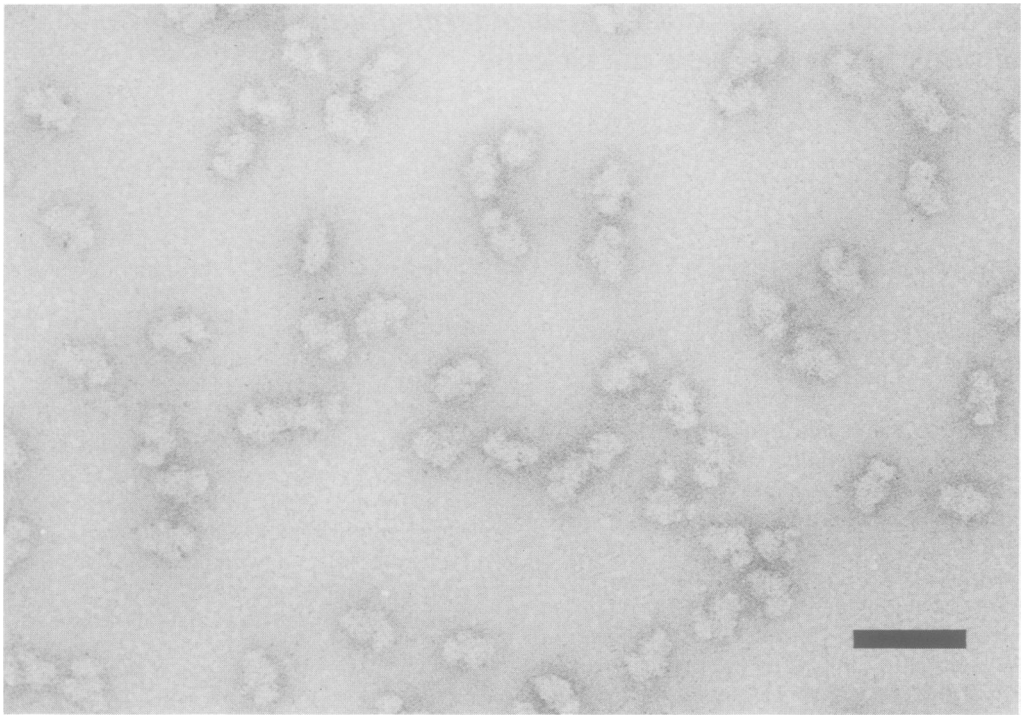

Fig. 1. Part of one of the original micrographs (*B. stearothermophilus*) used in the analysis. Bar represents 50 nm.

the small lobe is very prominent and there is an incision just below it (Figure 2B). These characteristic details are consistently connected by band-like structures inside the contour of the molecule (Figure 2A, B).

Escherichia coli

Contrary to the *B. stearothermophilus* data, the total sum of all *E. coli* aligned images was found to be mirror-symmetric, indicating that left- and right-handed versions of the *E. coli* particles in this preparation occur with the same frequencies and that there are no preferential staining effects towards either of the carbon foils. By including a full mirrored data set in the analysis, we arranged the multivariant statistical analysis (MSA) procedure such that right- and left-handed versions of the molecules could fall into the same class. Thus each class appears twice: once in its right- and once in its left-handed form. The 11 classes shown in Figure 4 are the left-handed versions only.

The predominant views of *E. coli* are the lateral view (25%, Figure 4a), the intermediate view (~40%, Figure 4B) and the quasi-symmetric views (25%, Figure 4C). The *E. coli* preparation shows a slightly more 'random' behaviour than the *B. stearothermophilus* preparation in that the predominant views of *E. coli* show a somewhat larger internal variation. The last lateral view in Figure 4A already resembles the intermediate view; the last intermediate view (Figure 4B) is already close to the quasi-symmetric projections. A statistically significant number of images of the compact and of the curved quasi-symmetric variants (Figure 2D, E) were, on the other hand, not found in this data set of 422 images.

The major features of the predominant class averages are consistently present in *B. stearothermophilus* and in the corresponding *E. coli* averages (Figure 5). The beak structure on the head of the lateral view of the small subunit (Figure 5A) is less dominant in *E. coli* than in *B. stearothermophilus*. The main difference between the two species is seen in the neck region of the lateral views: the cleft between the head and the small lobe is much more pronounced in *E. coli* than in *B. stearothermophilus* (Figure 5A).

Resolution between and within classes

To assess the reproducible resolution both within and between the classes obtained, we use the Fourier ring correlation (FRC) method (Figure 6), which allows us to find the reproducible resolution – or cross-resolution – between two images (Saxton and Baumeister, 1982; Van Heel *et al.*, 1982b). A value between 2.0 and 1.7 nm was typically found between closely related classes. To determine the reproducible resolution within a class, the class is split into two independent sub-averages which are compared by the FRC method. The internal resolution within the good classes is also found to be between 2.0 and 1.7 nm. Since the full class sums contain less noise than each half-sum, these resolution estimates are conservative.

The cross-resolution between two projection classes furthermore allows us to estimate a maximum angular distance between the two projections. The cross-resolution gradually deteriorates with increasing angular distance: whereas at very small angular distances two projections are identical up to very high spatial frequencies, at larger angular distances only the low-frequency information remains consistent. For two classes related by a cross-resolution of ~2.0 nm we can estimate – given the size of the object – the angular distance to be well within 8°, conservatively assuming all differences between both classes to be exclusively due to an orientational difference. This implies that the 30S ribosomal subunit not only shows just a few preferential positions, but also that there is very little rotational freedom of the particle around these stable positions. This result contradicts the assumption of other authors (Verschoor *et al.*, 1984).

The reproducible resolutions in our average images are higher than in previously published images of the ribosome structure due to the large data sets analysed, as well as to the precision of the automatic classification scheme. Even with 40S rat liver ribosomal subunit (Frank *et al.*, 1982) where the predominant

left and right lateral views can be sorted visually, the resolution in the averages was considerably lower (3.2 nm).

A spatial frequency resolution of 1.7 nm implies that single details of ~1 nm size should be interpretable. However, due to the low amount of power present in the higher spatial frequency range (lower curve in Figure 6), the smallest visible details in the averages are ~1.5 nm.

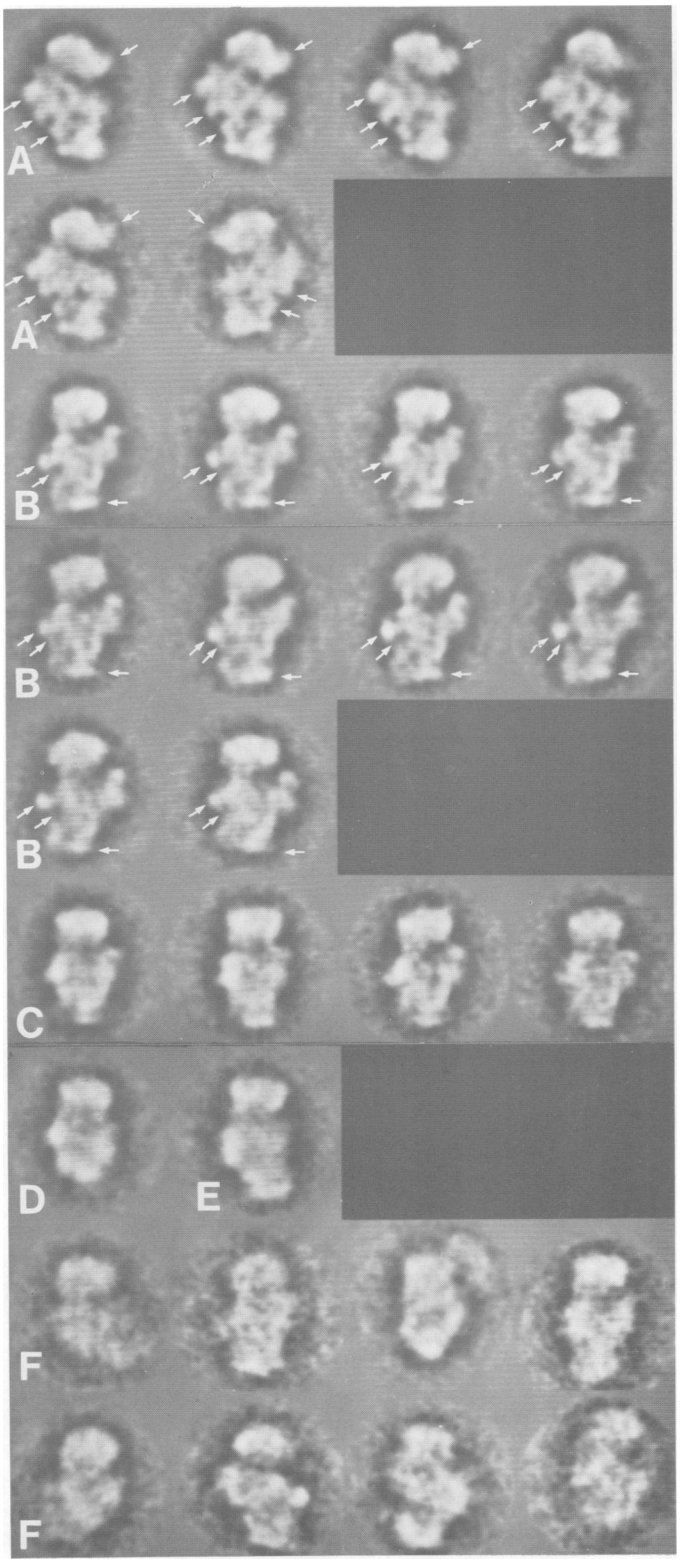

Discussion

In this study we found three to five stable positions for the 30S particle, and determined their averaged images with a resolution of up to 1.7 nm. This resolution range, in particular for the *B. stearothermophilus* images, is higher than in previous studies on ribosomal subunits. The resolution obtained in our single molecule analysis is comparable with that of negatively stained two-dimensional protein crystals [1.9 nm. in: (Saxton and Baumeister, 1982)]; in the case of two-dimensional crystals of the 50S ribosomal subunit (Clark *et al.*, 1982; Arad *et al.*, 1984), however, such a resolution has not yet been reached. One of the reasons for loss of high-resolution information in electron images of two-dimensional protein crystals is the loss of crystalline order as a function of electron dose. In single particle analysis this effect is non-existent, which may account for the relatively high resolution obtained in our study in spite of the high doses used (in excess of 200 electrons/Å^2)

The differences observed between the lateral view of *E. coli* and *B. stearothermophilus* are significant (Figure 5A). In view of the fact that hybrid 30S subunits can be reconstituted from rRNA and ribosomal proteins of the two species (Higo *et al.*, 1970), it appears unlikely that these differences reflect genuine structural differences between the ribosomes of the two bacterial species. More probably the differences are due to different adsorption of the 30S particles to the carbon foils. In this context, it is important to note that the lateral views of *E. coli* published by Verschoor *et al.* (1984) look more similar to our *B. stearothermophilus* lateral views than to our lateral views of *E. coli* (compare Figure 5 with Figure 2 of Verschoor *et al.*, 1984).

The lateral view of *B. stearothermophilus* has a marked resemblance to the lateral view of archaebacteria (Lake *et al.*, 1982) and of the 40S eukaryotic ribosomal subunit (cf. Figure 5A with: Boublik and Hellmann, 1978; Kiselev, 1980; Kiselev *et al.*, 1982; Frank *et al.*, 1981,1982). Among the new details visible is a beak in the head region of the *B. stearothermophilus* 30S particles. Although this beak is significantly shorter than the comparable feature in archaebacteria and eukaryotes, the mere presence of a beak is an insufficient criterion to differentiate between eubacteria and the other types (Henderson *et al.*, 1984).

The squarish base in the lateral view of *B. stearothermophilus* is also less prominent than in 40S subunits of eukaryotes; its size, however, attains that said to be exclusively found in sulfur-dependent archaebacteria (Henderson *et al.*, 1984). This structural feature is thus unsuitable as a phylogenetic marker, as proposed by Lake *et al.* (1982). A statistical analysis of a large number of electron microscopical images is necessary for an objective comparison of these fine structural details in the ribosomal subunits from different organisms.

Fig. 2. Classes found for *B. stearothermophilus*, representing 95% of the total population of images. The classes are sorted by characteristic views. The 'lateral' view **(A)** represents 32% of the population; the last lateral view is an exceptional left-handed view. The 'intermediate' view **(B)** which shows two arm-like protrusions, represents ~40% of the images; the last two of these classes are orientations which tend to the left-handed lateral view. The three other views that are found to be significant are the 'quasi-symmetric' view **(C**; 10%), the compact **(D**; 3%) and the curved variants **(E**; 3%) of the quasi-symmetric view. Arrows indicate characteristic details. For each characteristic view, the classes are sorted, mainly by number of members. **F** shows the bad classes with a high internal variance. The number of members per class are respectively: **A.** 80, 71, 49, 48, 18 and 21 members; **B:** 53, 38, 36, 33, 24, 24, 24, 23, 30 and 24 members; **C:** 33, 23, 15 and 15 members; **D:** 23 members; **E:** 27 members; and **F.** 17, 11, 31, 11, 19, 14, 20 and 13 members.

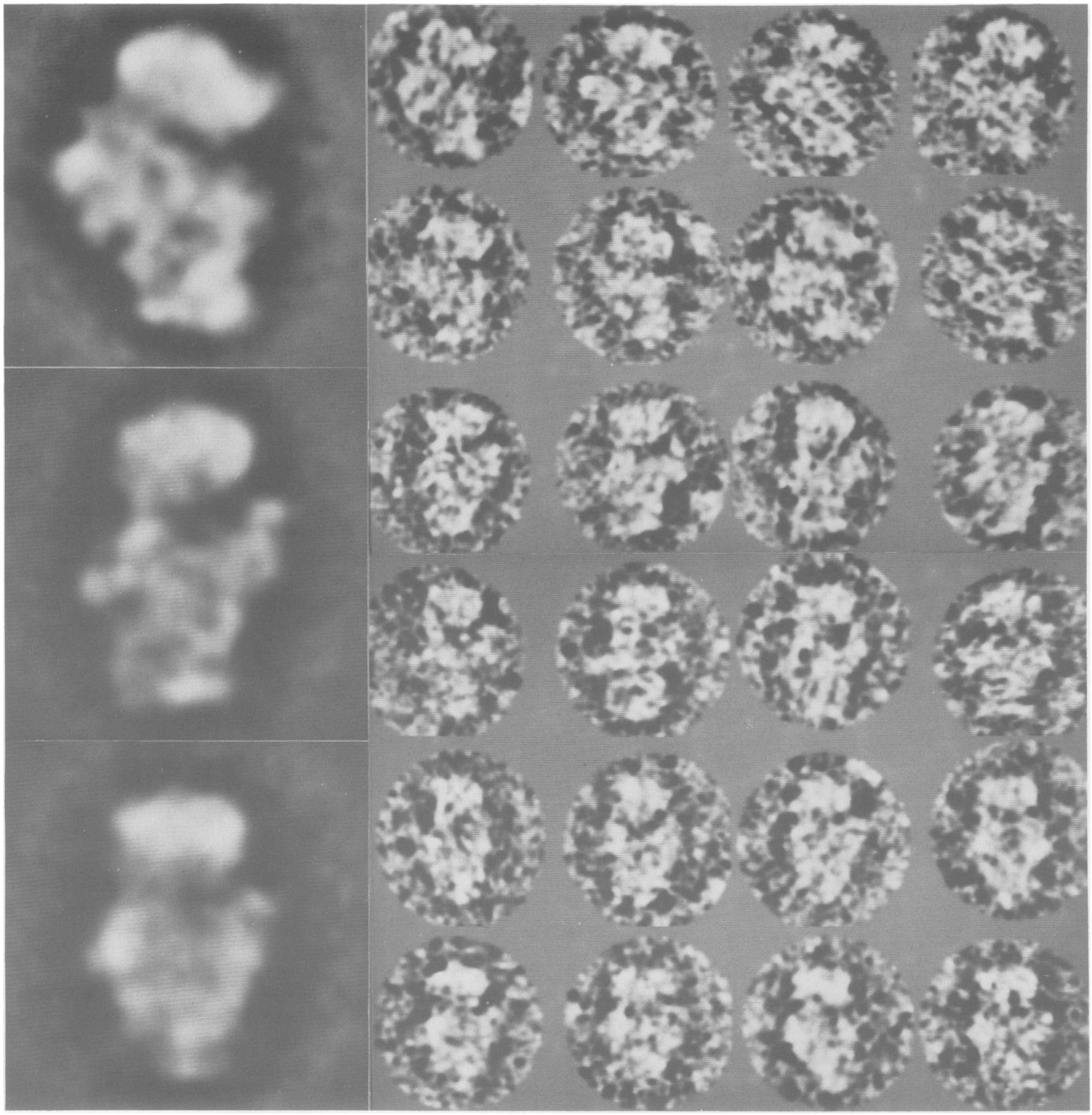

Fig. 3. Three typical class averages of *B. stearothermophilus* together with eight of the (aligned) original images chosen at random from the members of the classes, to demonstrate the sorting power of the technique. The noisy images originally appear unaligned and mixed together in the micrographs.

Our high-resolution class-averages may be used to derive better three-dimensional models for the bacterial ribosomal subunit. In the Lake model (1976), the lateral view was over-emphasized which led to a flat model with only one protrusion. The Boublik model and the Tischendorf model (Boublik *et al.*, 1977; Tischendorf *et al.*, 1975) on the other hand, emphasize the intermediate view, ignoring the lateral view. The models most consistent with our analysis of the electron microscopical data are that by Vasiliev (Shatsky *et al.*, 1979) and that by Stöffler (Stöffler and Stöffler-Meilicke, 1983; Stöffler-Meilicke *et al.*, 1984); for the latter model the three main views were taken into account.

In a recent paper (Verschoor *et al.*, 1984) a three-dimensional model of the 30S ribosomal subunit of *E. coli* was presented based on a MSA study of microscopical images. These authors excluded the lateral ('broad') views (30% of their images) from their three-dimensional analysis, considering them to be artefactual. However, the lateral view has been observed by many authors in 30S subunits from *E. coli* and this view compares with the most abundant view in small ribosomal subunits of both archaebacteria (Lake *et al.*, 1982) and eukaryotes (Boublik and Hellman, 1978; Henderson *et al.*, 1984). Verschoor and co-workers have themselves extensively studied this lateral view of 40S subunits

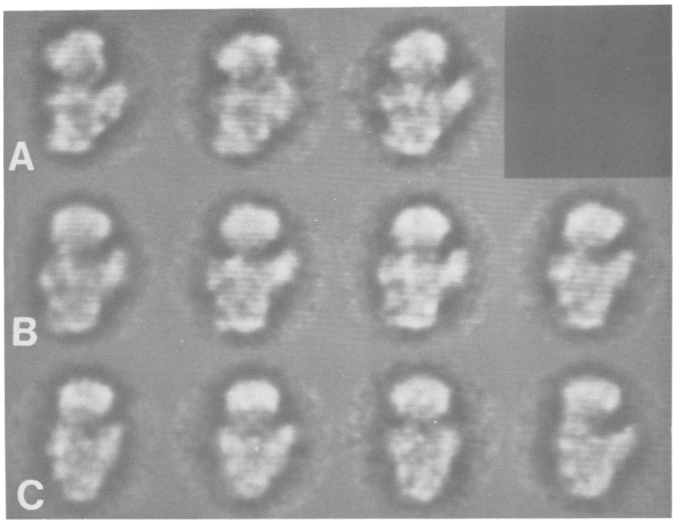

Fig. 4. Classes of *E. coli*, representing 90% of the total population of images. Main views are the 'lateral' view (**A**, 25%), the 'intermediate' view (**B**, 43%) and the 'quasi-symmetric' view (**C**, 29%). The last lateral view may represent a transition form towards the intermediate view. The number of members per class: **A.** 45, 28, 26; **B:** 67, 33, 32, 41; **C:** 32, 26, 23, 36; one bad class containing 19 members is not shown. Five percent of the images were automatically rejected during the classification.

from HeLa cells (Frank *et al.*, 1981, 1982). Of the remaining 160 molecular images a further 100 were excluded after the visual classification procedure. The nine classes actually used for the reconstruction are somewhat arbitrarily assigned equidistant angles over a 180° range. Those classes, however, correspond to our quasi-symmetrical and intermediate views, and thus reflect the molecule merely in two stable molecular orientations.

The low number of projections found in our study limits the attainable resolution in a three-dimensional reconstruction. Alternative preparation techniques such as ice-embedding allow for greater randomness in molecular orientations. The goniometer stage may also be used to obtain additional views from the molecules. More orientations, however, require the simultaneous analysis of a larger number of molecules to ensure the same statistical significance per class. More efficient algorithmic approaches are being developed to increase the practical limit for the analysis from the current 1100 molecules (2 weeks of calculation) by an order of magnitude.

The reproducible high resolution obtained demonstrates the sorting power of our MSA techniques, which shares the basic philosophy of noise reduction by averaging with the already classical crystallographic techniques. In our new technique the differences between images are treated with the same respect as the global average in the older technique, thus allowing the systematic analysis of non-uniform populations of images.

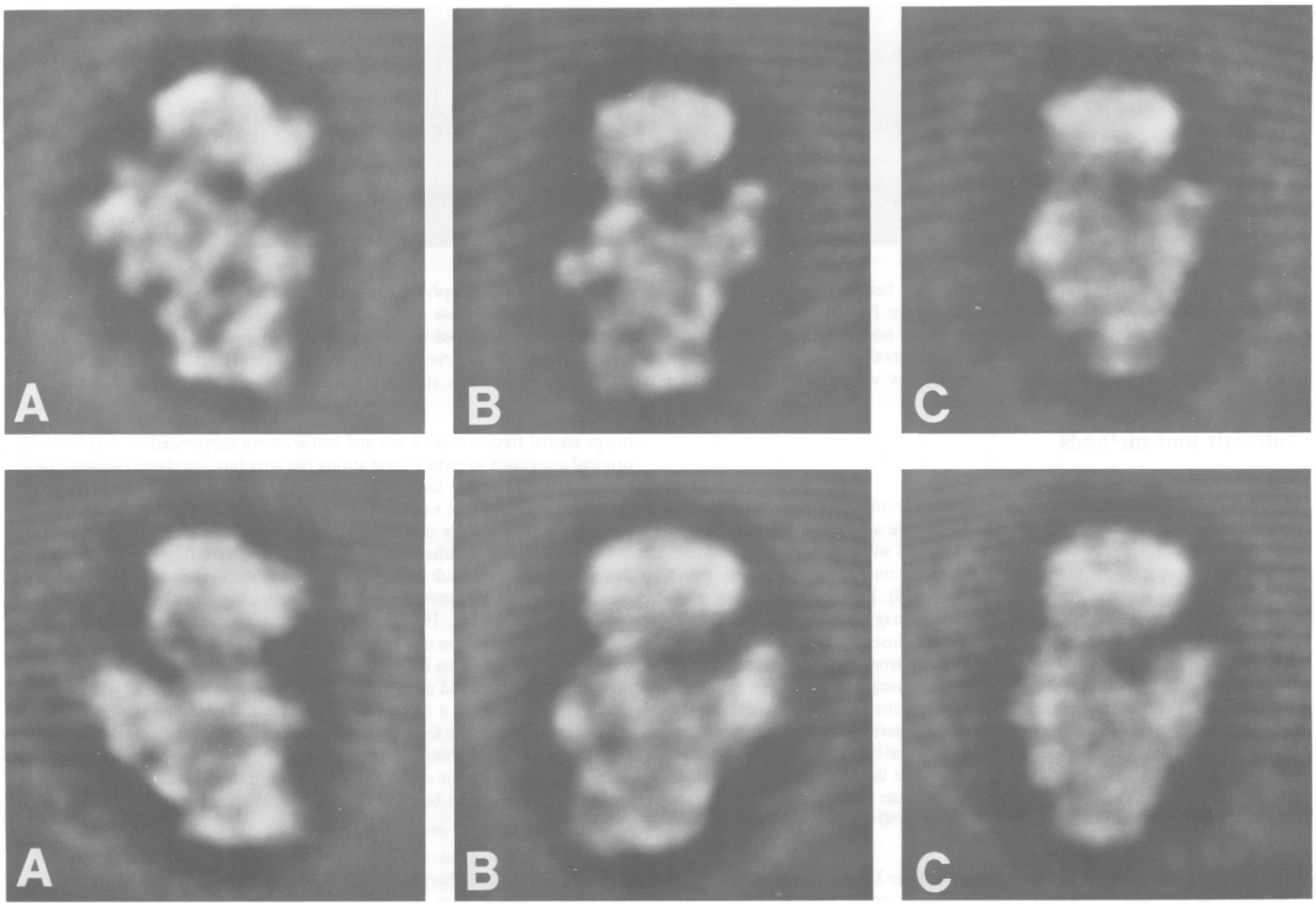

Fig. 5. The three predominant views for *B. stearothermophilus* (top) compared with those of *E. coli* (bottom); **(A)** lateral, **(B)** intermediate and **(C)** quasi-symmetric view. Gross features are similar in both species; however, significant differences are found, for example, in the 'neck' region of the lateral views.

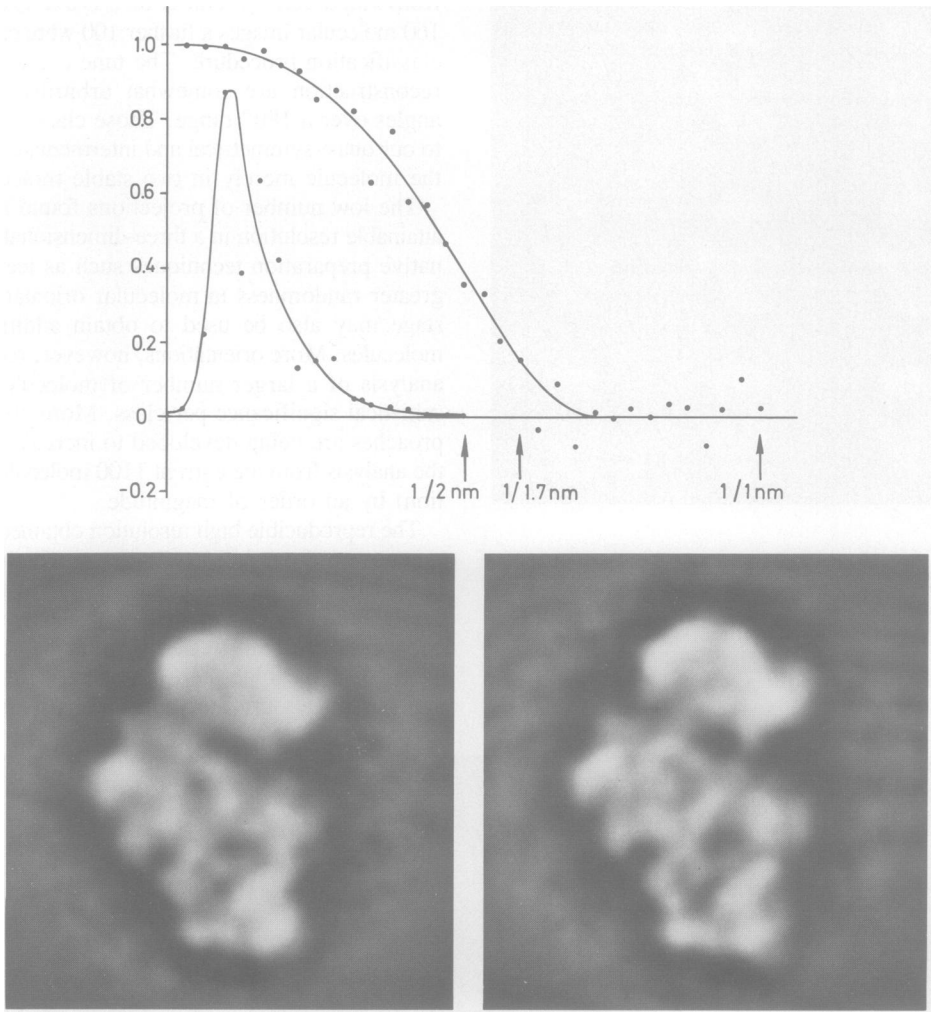

Fig. 6. A typical Fourier ring correlation function between two closely related classes of *B. stearothermophilus* images (Figure 2A-1 versus Figure 2A-2). The function is calculated by (conjugate) multiplying the Fourier components of two images and summing these over rings in Fourier space. The sums per ring are normalized by the square root of the power in the corresponding ring of each of the transforms. The cross-resolution (spatial frequency) between images is ~1.7 nm. This value was found between most lateral-view and intermediate-view classes. The power curve is a typical radial power spectrum curve of a good class. Although the radial power drops to low values beyond 2 nm, the Fourier ring correlation can still be significant due to the normalization.

Materials and methods

Data preparation

70S ribosomal tight couples from *E. coli* and *B. stearothermophilus* were isolated as described (Noll *et al.*, 1973). The 30S ribosomal subunits were isolated by zonal centrifugation (Hindennach *et al.*, 1971). 30S subunits were prepared for electron microscopy by the double-layer carbon technique and negatively contrasted with uranyl acetate (Tischendorf *et al.*, 1974). Electron microscopy was performed on a Philips EM 301 at an instrumental magnification of 110 000 and an accelerating voltage of 80 kV. The grids were inserted into the microscope with the specimen side oriented away from the electron source. No special procedure for low-dose microscopy was followed. Subsequent printing or negative enlarging was done with the plate emulsion facing the paper or negative emulsion. The micrographs were digitized (through intermediate enlargements on negative material) using an OPTRONICS rotating drum densitometer with a sampling aperture (and grid) corresponding to 0.50 nm at the object level. Eight different micrographs of the *E. coli* preparation and nine of *B. stearothermophilus* were used, each micrograph (Figure 1) containing 50 – 100 molecular images.

Multi-reference alignment

All image analysis was done in the framework of the IMAGIC software system (Van Heel and Keegstra, 1981) on a VAX-11/780 computer. All distinct molecules that were not overlapping or in close contact with other molecules were selected interactively from the digitized micrographs using a raster-scan image display system. A total of 422 molecules for *E. coli* and 914 for *B. stearothermophilus* were selected to ensure good statistical significance of the results. The single molecular images were normalized by the following procedure: (i) the very low image spatial frequencies (8 nm and below) were suppressed to ~1/20 of their original amplitude to reduce their strong but structure-unrelated influence on the further procedures; (ii) the images were then 'floated' to zero average density and given a normalised variance; (iii) the molecules were surrounded by a circular mask to cut away unnecessary background.

The individual molecules were aligned relative to 10 different references, which themselves were the result of earlier alignment-classification rounds in an iterative procedure known as 'multi-reference alignment technique' (MRA) (Van Heel, 1984b; Van Heel *et al.*, 1982a). We can only align molecular images using correlation methods (Saxton and Frank, 1977; Frank *et al.*, 1978) if they 'look like' the reference image. This implies that we need various (noise-free) 'characteristic images' to align a mixed population. Since these are the 'classes' which we seek to determine, we have a logical problem which can only be solved iteratively.

To reduce further the influence of the stain surrounding the molecules during alignment, reference images are surrounded by a narrow contour mask. After the alignment, a contour around the total sum of the images determines the image areas which are to be active during the MSA procedures.

Multivariate statistical analysis techniques

In the eigenvalue eigenvector technique known as correspondence analysis (J. P. Benzécri, 1980; Lebart *et al.*, 1977) a population of images is decomposed into a set of independent, orthogonal eigenimages (Frank and Van Heel, 1982; Van Heel, in preparation). The original images are then expressed as linear combinations of the (typically eight) most important eigenimages; i.e., those eigenimages that describe most of the variance in the data set. Since the images that were originally described by their typically 4096 (=64 × 64) density values are now expressed merely by eight coefficient ('factorial' coordinates), an enor-

mous reduction in the total amount of data is achieved, which facilitates the understanding of the information present in the images. A two-dimensional map showing the first two factorial coordinates of the images may be sufficient to distinguish classes of images (Van Heel and Frank, 1981). This visual approach is subjective and not reproducible, and becomes impossible to apply in more complicated situations where more than two or three significant eigenimages must be taken into account.

In this work we use the variance-oriented HAC scheme, which is appropriate when the molecule shows a limited number of stable positions (Van Heel, 1984a). In this scheme, we start with as many classes as there are images (each image is one class) and then, at any level of the procedure, merge those two classes which are closest together, until we finally obtain one big class containing all images. Two classes are merged if the resultant increase in the total intra-class variance (internal variance in a class) is the minimum possible at the given level of the classification (F. Benzécri, 1980; Van Heel, 1984a). The merging history is stored in a 'classification tree', and a partition can be obtained by cutting the tree at any particular level. The HAC procedure leads to a partition that is close to optimal in the sense that for the given number of classes the intra-class variance is low (Benzécri *et al.*, 1977; F. Benzécri, 1980).

As a refinement we then extract each original image from its class to see whether it would not fit better into a different class. If so, we place it into that other class and continue with the next image; the refinement procedure is iterated until no further migrations of images between classes occur. This refinement led to a decrease of ~10% in the total intra-class variance. An additional (automatic) decision is the exclusion of a certain percentage of the 'worst' images from the classification. Those images are considered bad which were the last individuals to be placed into a class in the HAC procedure; this implies that their merging into the class was associated with a large increase of intra-class variance. We typically rejected ~5% of the original images using this criterion. The bad images are either misaligned molecules or uncharacteristic images which appear only once in a large population. The first two coordinates of the images were weighted down during the classification following the standard weighting scheme (Van Heel, 1984a) whereas the remaining six coordinates received a unit weight.

Acknowledgements

We would like to thank V. Fijala for doing part of the image analysis, R. Albrecht-Ehrlich for taking the micrographs, and Dr. G. Harauz for comments on the manuscript. We also thank Drs. E. Zeitler, H. G. Wittmann and G. Stöffler for their continuous support of the project. MvH was recipient of EMBO fellowship ALTF-99-1982; MSM is recipient of a DFG fellowship (SFB-9).

References

Arad,T., Leonard,K., Wittmann,H.G. and Yonath,A. (1984), *EMBO J.*, **3**, 127-131.

Benzécri,F. (1980) *Les Cahiers de L'Analyse des Données*, **5**, 311-340.

Benzécri,J.-P. (1980) *L'Analyse des Données, Vol 2: L'Analyse des Correspondances*, published by Dunod, Paris.

Benzécri,J.-P., Danech Pejouh,M., Moussa,T. and Romeder,J.-P. (1977) *Les Cahiers de l'Analyse des Données*, **4**, 369-406.

Boublik,M. and Hellmann,W. (1978) *Proc. Natl. Acad. Sci. USA*, **75**, 2825-2933.

Boublik,M., Hellmann,W. and Kleinschmidt,A.K. (1977) *Cytobiologie*, **14**, 293-300.

Clark,M.W., Leonard,K. and Lake,J. (1982) *Science (Wash.)*, **216**, 999-1001.

DeRosier,D.J. and Klug,A. (1968) *Nature*, **217**, 130-134.

Frank,J. and Van Heel,M. (1982) *J. Mol. Biol.*, **161**, 134-137.

Frank,J., Goldfarb,W., Eisenberg,D. and Baker,T.S. (1978) *Ultramicroscopy*, **3**, 283-290.

Frank,J., Verschoor,A. and Boublik,M. (1981) *Science (Wash.)*, **214**, 1353-1355.

Frank,J., Verschoor,A. and Boublik,M. (1982) *J. Mol. Biol.*, **161**, 107-137.

Henderson,E., Oakes,M., Clarck,M.W., Lake,J.A. Matheson,A.T. and Zillig,W. (1984) *Science (Wash.)*, **225**, 510-512.

Higo,K., Held,W., Kahan,L. and Nomura,M. (1970) *Proc. Natl. Acad. Sci. USA*, **70**, 944-948.

Hindennach,I., Stöffler,G. and Wittmann,H.G. (1971) *Eur. J. Biochem.*, **23**, 7-11.

Kiselev,N.A. (1980) *Proceedings of the 7th European Congress on Electron Microscopy, The Hague*, Vol. **2**, pp. 572-579.

Kiselev,N.A., Ste'mashchuk,V.Ya., Orlova,E.V., Platzer,M., Noll,F. and Bielka,H. (1982) *Mol. Biol. Rep.*, **8**, 185-189.

Lake,J.A. (1976) *J. Mol. Biol.*, **105**, 131-159.

Lake,J.A., Henderson,E., Clark,M.W. and Matheson,A.T. (1982) *Proc. Natl. Acad. Sci. USA*, **79**, 5948-5952.

Lebart,L., Morineau,A. and Tabard,N. (1977) *Techniques de la Description Statistique*, published by Dunod, Paris.

Noll,M., Hapke,B., Schreier,M.H. and Noll,H. (1973) *J. Mol. Biol.*, **75**, 281-294.

Saxton,W.O. and Frank,J. (1977) *Ultramicroscopy*, **2**, 219-227.

Saxton,W.O. and Baumeister,W. (1982) *J. Microsc.*, **127**, 127-138.

Shatsky,I.N., Mochalova,L.V., Kojouharova,M.S., Bogdanov,A.A. and Vasiliev,V.D. (1979) *J. Mol. biol.*, **133**, 501-515.

Stöffler,G. and Stöffler-Meilicke,M. (1983) in Tschesche,H. (ed.), *Modern Methods in Protein Chemistry* – Review Articles, De Gruyter & Co., Berlin, NY, pp. 409-455.

Tischendorf,G.W., Zeichardt,H. and Stöffler,G. (1974) *Mol. Gen. Genet*, **134**, 209-223.

Tischendorf,G.W., Zeichhardt,H. and Stöffler,G. (1975) *Proc. Natl. Acad. Sci. USA*, **72**, 4820-4825.

Unwin,P.N.T. and Henderson,R. (1975) *J. Mol. Biol.*, **94**, 425-440.

Van Heel,M. (1984a) *Ultramicroscopy*, **13**, 165-183.

Van Heel,M. (1984b) *Proceedings of the 8th European EM Conference*, Budapest, pp. 1317-1325.

Van Heel,M. and Frank,J. (1981) *Ultramicroscopy*, **6**, 187-194.

Van Heel,M. and Keegstra,W. (1981), *Ultramicroscopy*, **7**, 113-130.

Van Heel,M., Bretaudière,J.P. and Frank,J. (1982a) *Proceedings of the 10th International Congress on Electron Microscopy*, Vol. **1**, Hamburg, pp. 563-564.

Van Heel,M., Keegstra,W., Schutter,W. and Van Bruggen,E.F.J. (1982b) in Wood,E.J. (ed.), *Life Chemistry Reports, Suppl. 1, The Structure and Function of Invertebrate Respiratory Proteins*, EMBO workshop, Leeds 1982, pp. 69-73.

Verschoor,A., Frank,J., Radermacher,M., Wagenknecht,T. and Boublik,M. (1984) *J. Mol. Biol.*, **178**, 677-698.

Received on 19 April 1985; revised on 13 June 1985

Note added in proof

After submission of this manuscript, a paper has been published by Lake *et al.* [(1985) *Proc. Natl. Acad. Sci. USA*, **82**, 3716-3720], in which the authors claim that a split platform and a gap below it are characteristic only for small ribosomal subunits from methanogenic archaebacteria, sulfur-metabolizing archaebacteria and from eukaryotes, and that these features are lacking in the so-called 'photocytes', which comprise eubacteria and halophilic archaebacteria. In our paper we demonstrate that the lateral views of the eubacterium *B. stearothermophilus* show these same structural details (Figures 2A, 5A and 6B). As will be discussed in more detail elsewhere (G. Stöffler and M. Stöffler-Meilicke, *System. Appl. Microbiol.*, in press), this illustrates once more that fine structural details observed in images of ribosomal subunits should not be used to demarcate phyla or kingdoms.